An accurate coupling efficiency evaluation for high-order modes based on Laguerre-Gaussian modes

1st Feng Liu
College of electrical and electronic engineering
Wenzhou University
Wenzhou, China
liufeng@wzu.edu.cn

2nd Mengmeng Cai
College of electrical and electronic engineering
Wenzhou University
Wenzhou, China
21211764251@stu.wzu.edu.cn

3rd Tianle Gu
College of electrical and electronic engineering
Wenzhou University
Wenzhou, China
22451841009@stu.wzu.edu.cn

***Abstract*—In this paper, based on a scale-adapted set of Laguerre-Gaussian modes, a theoretical model has been presented for evaluating the coupling efficiency between high-order modes of few mode fibers caused by transverse and angular misalignments. A proof-of-model demonstration is performed for six mode fiber, and the results show that the coupling efficiency of various high-order modes behaves differently in the presence of axial offset and the direction of the misalignment.**

Keywords—Few mode fiber, coupling efficiency, fusion splice loss, higher order mode

I. INTRODUCTIO N

With the continuous increase of communication services, the demand for transmission capacity of communication systems is increasing, and various new technologies are emerging. Currently, Few Mode Fiber (FMF) communication technology based on Mode Division Multiplexing (MDM) is favored [1-4]. This technology can break through the capacity limit of traditional single mode optical fiber (SMF) communication by mining the new degree of freedom of mode as an independent channel for information transmission. It is the most competitive expansion scheme to solve the "bandwidth crisis" of future communication networks, and becomes the key to achieving future T bit/s or even P bit/s optical fiber communication. In the face of the rapid development of research and development, network construction, and application of FMF, ensuring the reliable and efficient operation, analysis of the fusion splice efficiency evaluation of a FMF link has become extremely important [5].

In a MDM system based on FMF, fusion splice between FMFs is inevitable. For the FMF, which supports multiple spatial modes and each spatial mode has a large difference in transmission loss characteristics, the precise analysis of high-order spatial mode coupling loss characteristics of FMF fusion splice faults can provide a reliable basis for evaluating fusion quality and fault detection sensitivity. At present, many achievements have been reported on the analysis of coupling efficiency of FMF fusion faults. ATSUSHI NAKAMURA et al. proposed a novel technique based on OTDR for characterizing the losses of LP_{01} and LP_{11} modes along FMFs, and estimated the coupling efficiency matrix at the fusion splice point by using the Rayleigh backscattering waveform of each spatial mode. Waveforms that are free from the crosstalk influence enable us to obtain the true losses independently of the crosstalk-inducing point [6]. Hiroshi Takahashi et al. reported a method for measuring the modal attenuation of the splice loss of a purely LP_{11} mode group by using OTDR with a dynamic modal crosstalk suppression technique based on Brillouin loss mechanism for FMFs. The degradation of LP_{11} mode fault loss measurement accuracy under mode crosstalk conditions has been effectively resolved [7]. Atsushi Nakamura et al. approximated the field intensity distribution of LP_{01} and LP_{11} modes of FMF by Gaussian and Hermite-Gaussian expressions, respectively, and analyzed the efficiency characteristics of the fusion splice coupling efficiency between modes [8]. Atsushi Nakamura et al. determined whether the loss was due to large bending or fusion splicing by evaluating the ratio of loss occurring in the LP_{01} and LP_{11} modes of backscattered light [9]. In previous work, we discussed the influence mechanism of mode crosstalk on fusion loss and fault detection sensitivity characteristics of LP_{01} and LP_{11} under different fusion splice mismatch and rotation conditions [10]. However, the above report has analyzed the fusion loss characteristics of the fundamental modes LP_{01} and LP_{11} of FMF, and no further research has been conducted on the coupling efficiency of higher order spatial mode for FMF, resulting in a lack of corresponding theoretical basis.

In this paper, a general theoretical model for the coupling efficiency at the fusion splice point of high order spatial modes is established. Taking a 6-mode optical fiber as an example, the coupling efficiency of each spatial mode is analyzed under the conditions of parameters. The coupling efficiency of different spatial modes under the influence of different welding parameters is compared and verified by numerical calculation. The simulation results show that the theoretical model can be used to accurately analyze the coupling efficiency of high-order spatial mode.

II. THEORETICAL INVESTIGATION

In practice, fusion splice is essential in a FMF link. Here, we consider the fusion splice of two such FMF with matched parameters, as shown in Fig.1, i.e. the two FMFs are assumed to have same core radii a, relative-index Δ, normalized frequencies V as well as profile shapes. When transmitting and receiving FMFs are fused, there will be the axial offset d and direction misalignment θ. x and y are coordinates on the cross section of the FMF, and $r^2 = x^2 + y^2$. z indicates the axial direction of FMF.

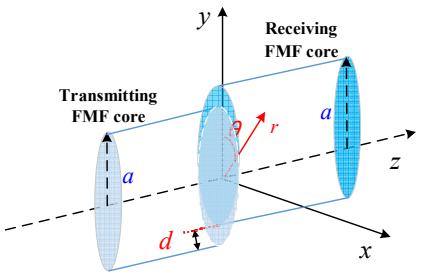

Fig.1. Cross section of fusion splice with axial and direction misalignment.

Since the step-index fiber has cylindrical symmetry, and this cylindrical symmetry can be also defined as LG modes. So，the fields for the modes can be approximated by a scale-adapted set of Laguerre-Gaussian modes, and the solution of LG modes can be represented as[11]：

$$LG_{pl}(r,\theta)=\frac{A_{pl}}{\omega_0}\left(\frac{2r^2}{\omega_0^2}\right)^{\frac{1}{2}}L_p^l\left(\frac{2r^2}{\omega_0^2}\right)\exp\left(-\frac{r^2}{\omega_0^2}\right)e^{-il\theta} \quad (1)$$

where $A_{pl}=\left[\frac{2p!}{\pi(p+1)!}\right]^{\frac{1}{2}}$ is a normalization factor, and where l and p are the indices for the guided azimuthal and radial components. L_p^l are the associated Laguerre polynomials. $\omega_0=\sqrt{a/\left(kn_1\sqrt{2\Delta}\right)}$ is the fundamental Gaussian radius, k is wavenumber, Δ is relative-index, n_1 is core refractive index. Here, we consider an optical fiber that supports the LP_{01}, LP_{11} (degenerate spatial modes LP_{11a} and LP_{11b}), LP_{21} (degenerate spatial modes LP_{21a} and LP_{21b}), and LP_{02} mode. According to Eq. (1), the field intensity distribution of each spatial mode can be approximated by LG mode as follows:

$$E_{01}=\sqrt{\frac{2}{\pi\omega_0^2}}\exp\left(-\frac{x^2+y^2}{\omega_0^2}\right) \quad (2)$$

$$E_{11a}=\sqrt{\frac{4}{\pi\omega_0^4}}x\exp\left(-\frac{x^2+y^2}{\omega_0^2}\right) \quad (3)$$

$$E_{11b}=\sqrt{\frac{4}{\pi\omega_0^4}}y\exp\left(-\frac{x^2+y^2}{\omega_0^2}\right) \quad (4)$$

$$E_{21a}=\sqrt{\frac{4}{\pi\omega_0^6}}\left(x^2-y^2\right)\exp\left(-\frac{x^2+y^2}{\omega_0^2}\right) \quad (5)$$

$$E_{21b}=\sqrt{\frac{4}{\pi\omega_0^6}}2xy\exp\left(-\frac{x^2+y^2}{\omega_0^2}\right) \quad (6)$$

$$E_{02}(r,\varphi)=\sqrt{\frac{2}{\pi\omega_0^2}}\left[1-\frac{2\left(x^2+y^2\right)}{\omega_0^2}\right]\exp\left(-\frac{x^2+y^2}{\omega_0^2}\right) \quad (7)$$

As shown in Fig.1, under the conditions of axial offset d and direction misalignment θ for the fusion slice of FMF, the coupling efficiency η_{ij} between the LP_i mode and the LP_j mode ($i,j=1,2,3,L,6$ respectively represent modes 01, 11a, 11b, 21a, 21b, and 02) at the fusion splice point can be estimated by the overlapping integral of the electric field intensity distribution,

$$\eta_{ij}=\frac{\left|\iint E_i(x,y)E_j(x-d\cos\theta,y-d\sin\theta)dxdy\right|^2}{\iint E_i^2(x,y)dxdy\iint E_j^2(x,y)dxdy} \quad (8)$$

where η_{ij} is the coupling efficiency between the two modes at the fusion splice point of the FMF, reflecting the power coupling degree. By substituting Eq. (2) - (7) into Eq. (8), the coupling efficiency expressions of LP_{01}, LP_{11a}, LP_{11b}, LP_{21a}, LP_{21b} and LP_{02} modes can be obtained, as shown in Table 1.

TABLE I. MATHEMATICAL MODELS OF THE COUPLING EFFICIENCY OF FMF SPATIAL MODE

η_{ij}	LP_{01}	LP_{11a}	LP_{11b}	LP_{21a}	LP_{21b}	LP_{02}
LP_{01}	χ	$\frac{d^2\cos^2\theta}{\omega_0^2}\cdot\chi$	$\frac{d^2\sin^2\theta}{\omega_0^2}\cdot\chi$	$\frac{d^4\cos^2(2\theta)}{4\omega_0^4}\cdot\chi$	$\frac{d^4\cos^2(\theta)\cdot\sin^2(\theta)}{\omega_0^4}\cdot\chi$	$\frac{d^4}{4\omega_0^4}\cdot\chi$
LP_{11a}		$\frac{\left(\omega_0^2-d^2\cos^2\theta\right)^2}{\omega_0^4}\cdot\chi$	$\frac{d^2\cos^2\theta\sin^2\theta}{\omega_0^4}\cdot\chi$	$\frac{d^2\cos^2\theta\left(2\omega_0^2-d^2\cos^2 2\theta\right)^2}{4\omega_0^6}\cdot\chi$	$\frac{d^2\left(\omega_0^2-d^2\cos^2\theta\right)^2\sin^2\theta}{\omega_0^6}\cdot\chi$	$\frac{d^2\left(2\omega_0^2-d^2\right)^2\cos^2\theta}{4\omega_0^6}\cdot\chi$
LP_{11b}			$\frac{\left(\omega_0^2-d^2\sin^2\theta\right)^2}{\omega_0^4}\cdot\chi$	$\frac{d^2\left(2\omega_0^2+d^2\cos 2\theta\right)^2\sin^2\theta}{4\omega_0^6}\cdot\chi$	$\frac{d^2\left(\omega_0^2-d^2\sin^2\theta\right)^2\cos^2\theta}{\omega_0^6}\cdot\chi$	$\frac{d^2\left(d^2-2\omega_0^2\right)^2\sin^2\theta}{4\omega_0^6}\cdot\chi$
LP_{21a}				$\frac{\left(d^4-8d\omega_0^2+8\omega_0^4+d^4\cos 4\theta\right)^2}{64\omega_0^8}\cdot\chi$	$\frac{d^8\cos^2\theta\cdot\cos^2 2\theta\cdot\sin^2\theta}{4\omega_0^8}\cdot\chi$	$\frac{d^4\left(4\omega_0^2-d^2\right)^2\cos^2 2\theta}{16\omega_0^8}\cdot\chi$
LP_{21b}					$\frac{\left(\omega_0^2-d^2\cos^2\theta\right)^2\left(\omega_0^2-d^2\sin^2\theta\right)^2\cos^2 2\theta}{\omega_0^8}\cdot\chi$	$\frac{d^4\left(d^2-4\omega_0^2\right)^2\cos^2\theta\cdot\sin^2\theta}{4\omega_0^8}\cdot\chi$
LP_{02}						$\frac{\left(d^2-2\omega_0^2\right)^4}{16\omega_0^8}\exp\left(-\frac{d^2}{\omega_0^2}\right)$

According to the coupling mathematical model between different spatial modes at the fusion splice point in Table 1, the coupling efficiency can be estimated as a function of ω_0, d, and θ. χ is short for $\exp\left(-\frac{d^2}{\omega_0^2}\right)$. At the same time, due to the coupling symmetry between the modes, it can be calculated from Eq. (8) that $\eta_{ij}=\eta_{ji}$. When $i=j$, η_{ij} represents the mode coupling loss characteristics. The smaller the coupling efficiency of η_{ij}, the greater the power loss at fusion point, and vice versa. When $i\neq j$, η_{ij} represents the coupling loss characteristics. Represents the energy of LP_i mode coupling into LP_j mode. The greater the value of η_{ij}, the greater the crosstalk at the fusion point, and vice versa. There are some differences in coupling loss and coupling efficiency among different spatial modes.

III. NUMERICAL RESULTS AND DISCUSSIONS

In this section, theoretical analysis and numerical simulation are conducted based on above coupling efficiency model for FMF, and the coupling efficiency between each spatial mode are calculated. The correlation between the coupling efficiency and the axial offset (0~3μm) and the migration direction (0°, 45° and 90°) is calculated and analyzed. We use six-mode FMF (holding LP_{01}, LP_{11}, LP_{21}

and LP_{02} modes) as representatives. The refractive index of FMF core is 1.44979, cladding refractive index is 1.44402, optical wavelength lambda is 1550 nm, FMF core diameter is 18.5 μm.

(a) Coupling efficiencies between LP_{01} and higher order modes

According to the coupling efficiency mathematical model in the first row of Table 1, the coupling loss of LP_{01} mode at the fusion splice point can be obtained. At the same time, the coupling efficiency between LP_{01} mode and other higher-order modes can be calculated. As shown in Fig. 2 (a) the variation curve of self-coupling efficiency with axial offset when the fundamental mode LP_{01} of FMF is excited. It can be seen concluded that the coupling efficiency of LP_{01} mode decreases monotonically with the increase of d . since the field distribution of the LP_{01} mode is axially symmetric, η_{11} takes the same value for the misalignment directions of 0, 45 and 90 degrees. Figs. 2 (b) - (f) show the distribution of mode coupling efficiency between LP_{01} and LP_{11a}, LP_{11b}, LP_{21a}, LP_{21b}, and LP_{02} modes with axial offset and misalignment direction, respectively. The pink, green, and blue lines represent the results of misalignment direction of 0, 45 and 90 degrees, respectively.

As can be seen from Fig. 2 (b), under the same fusion offset condition, the coupling efficiency η_{12} decreases as the misalignment directions increase, and η_{12} is 0 at 90 degrees. Under the conditions of misalignment direction of 45 and 90 degrees, the coupling efficiency increases as the offset d increases. Similar conclusions exist between LP_{01} and LP_{11b} modes. The main difference is that coupling efficiency is switched under misalignment direction of 0 and 90 degrees, as shown in Fig. 2 (c), mainly because LP_{11a} and LP_{11b} are degenerate mode.

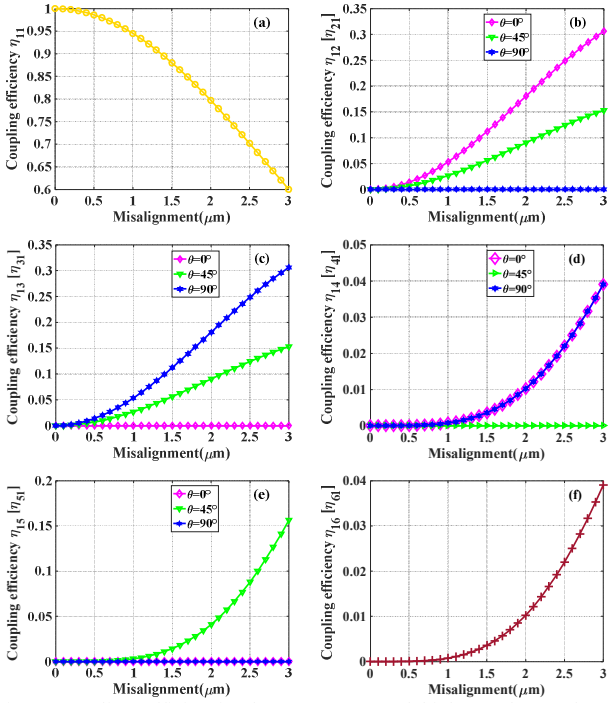

Fig.2. Coupling efficiencies between LP_{01} and higher order modes as a function of the axial misalignment. (a) self-coupling efficiency of LP_{01} mode; (b) ~(f) Coupling efficiencies between LP_{01} and LP_{11a}, LP_{11b}, LP_{21a}, LP_{21b}, and LP_{02} modes, respectively.

According to Fig. 2 (d), under the condition of misalignment direction of 45 and 90 degrees, the coupling efficiency of LP_{01} and LP_{21a} modes is the same, and increases with the increase of the fusion offset. When the misalignment direction is 45 degrees, the coupling efficiency is zero, while for the degenerate mode LP_{21b}, as shown in Fig.2 (e), the coupling efficiency η_{15} increases with the increase of the fusion offset, while the misalignment direction of 45 and 90 degrees, the coupling efficiency is zero. As shown in Fig. 2 (f), η_{16} and η_{61} take the same value for the misalignment directions of 0, 45 and 90 degrees, since the field distribution of the LP_{02} mode is axially symmetric, and as the offset increases, the coupling efficiency between LP_{01} and LP_{02} increases.

(b) Coupling efficiencies between LP_{11} and higher order modes

Similarly, according to Table 1, when LP_{11} mode (LP_{11a} and LP_{11b} mode) is excitation mode, the coupling efficiency of LP_{11} mode itself, and the coupling efficiencies between LP_{11} mode and other higher-order modes at the fusion point can be calculated. As shown in Fig. 3 (a), the coupling efficiency of LP_{11a} mode decreases monotonically with the increase of offset d , and the coupling efficiency increases with the increase of misalignment directions, while the degenerative mode LP_{11b} is completely opposite to LP_{11a}, as shown in Fig. 4 (a). According to Fig. 3(b), under the condition of misalignment directions of 0 and 90 degrees, the mode coupling efficiency between LP_{11a} and LP_{11b} is the same, and the value of η_{23} is 0. When the misalignment direction is 45 degrees, the coupling efficiency increases with the increase of the fusion offset.

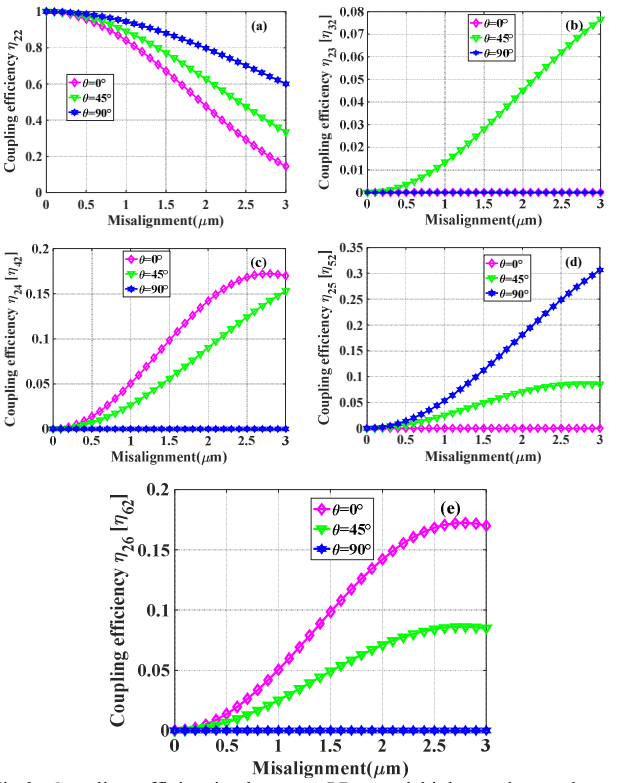

Fig.3. Coupling efficiencies between LP_{11a} and higher order modes as a function of the axial misalignment. (a) self-coupling efficiency of LP_{11a} mode; (b) ~(e) Coupling efficiencies between LP_{11a} and LP_{11b}, LP_{21a}, LP_{21b}, and LP_{02} modes, respectively.

As shown in Fig 3 (c), under the condition of misalignment direction of 0 and 45 degrees, the coupling efficiency increases with the increase of the fusion offset d , while fort the 0 degrees, the coupling efficiency decreases with the offset d reaching a certain degree. For misalignment directions of 90 degrees, the coupling coefficient is 0. The coupling efficiency between LP_{11b} and LP_{21a} presents this rule at 90 degrees, and η_{34} is 0 in misalignment directions of 0 degrees, as shown in Fig. 4 (b). The coupling efficiency between LP_{11a}, LP_{11b} and LP_{21b} is shown in Fig. 3 (d) and 4 (c), respectively. When the misalignment direction is 45 degrees, as the fusion offset reaches a certain degree, the coupling efficiency shows a downward trend. Moreover, due to the degeneracy mode, the η_{25} under 0 and 90 degrees is equal to η_{35} under fusion condition 90 and 0 degrees, respectively. The coupling efficiency between LP_{11a} and LP_{02} modes is shown in Fig. 3 (e). Under misalignment direction of 0 and 45 degrees, the coupling efficiency increases as the fusion offset increases, and as the offset reaches a certain degree, the coupling efficiency presents a downward trend. The same rule exists between LP_{11b} and LP_{02} under misalignment direction of 45 and 90 degrees.

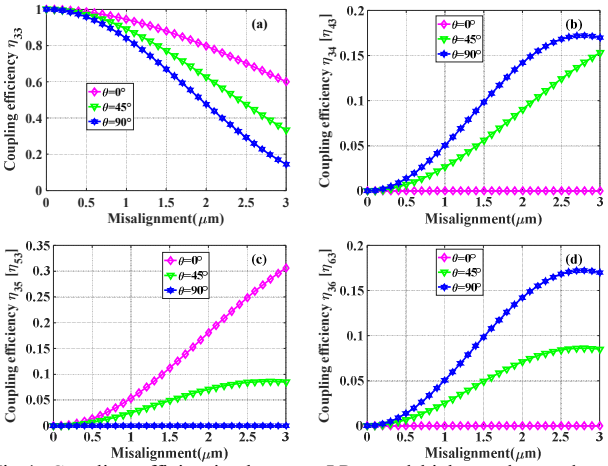

Fig.4. Coupling efficiencies between LP_{11b} and higher order modes as a function of the axial misalignment. (a) Self-coupling efficiency of LP_{11b} mode; (b) ~(d) Coupling efficiencies between LP_{11b} and LP_{21a}, LP_{21b}, and LP_{02} modes, respectively.

(c) Coupling efficiencies between LP_{21} and higher order modes

Figs. 5 and 6 show the coupling efficiency of LP_{21a} and LP_{21b} modes themselves, as well as the coupling efficiency with other higher order modes. As shown in Fig. 5 (a), the self-coupling efficiency of the LP_{21a} mode at the fusion point decreases monotonically with increasing offset d . The trend is consistent under misalignment direction of 0 and 90 degrees with that of the fusion joint conditions, and the coupling efficiency decreases faster under misalignment direction of 45 degrees. For LP_{21b} mode, the coupling efficiency is 0 at misalignment direction of 45 degrees, as shown in Fig. 6 (a). The coupling efficiency between degenerate modes LP_{21a} and LP_{21b} is 0 under misalignment direction of 0, 45, and 90 degrees, as shown in Fig. 5(b).

The calculation results of the mode coupling efficiency between LP_{21a} and LP_{02}, LP_{21b} and LP_{02} are shown in Figs. 5 (c), and 6 (b), respectively. The coupling efficiency between LP_{21a} and LP_{02} modes increases as the fusion offset increases at 0 and 90 degrees, while it is 0 at 45 degrees. As for the coupling efficiency between LP_{21b} and LP_{02} modes, only at misalignment directions of 45 degrees, η_{56} increases as the fusion offset increases. While at 0 and 90 degrees it is 0. The reason lies in the degeneracy between LP_{21a} and LP_{21b}.

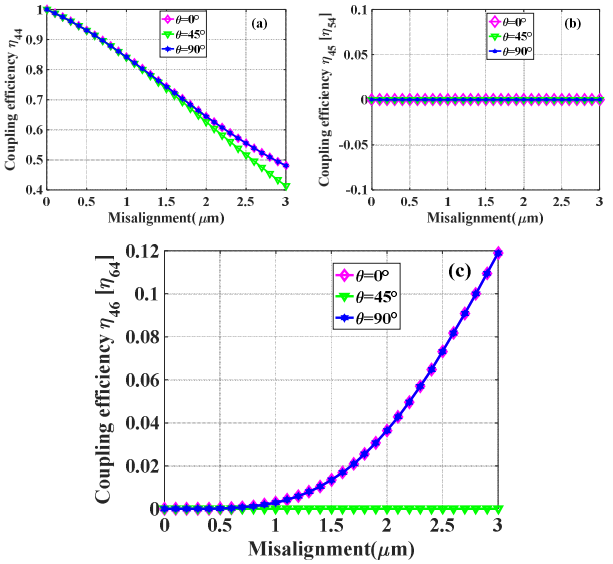

Fig.5. Coupling efficiencies between LP_{21a} and higher order modes as a function of the axial misalignment. (a) Self-coupling efficiency of LP_{21a} mode; (b) and (c) Coupling efficiencies between LP_{21a} and LP_{21b}, and LP_{02} modes, respectively.

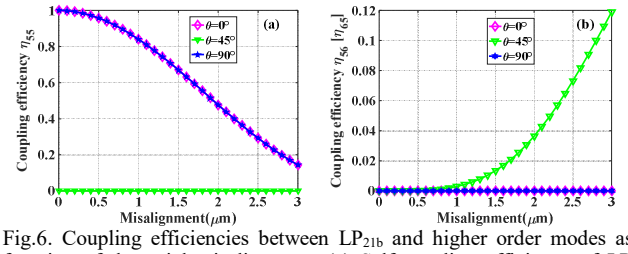

Fig.6. Coupling efficiencies between LP_{21b} and higher order modes as a function of the axial misalignment. (a) Self-coupling efficiency of LP_{21b} mode; (b) Coupling efficiencies between LP_{21b} and LP_{02} modes.

(d) Coupling efficiencies of between LP_{02} mode

As shown in Fig. 7, when the mode LP_{02} of a few mode optical fiber is excited, the self-coupling efficiency varies with the lateral offset. From the figure, it can be seen that the coupling efficiency of the LP_{02} mode monotonically decreases as d increases. η_{66} takes the same value for the misalignment directions of 0, 45 and 90 degrees, since the field distribution of the LP_{02} mode is axially symmetric.

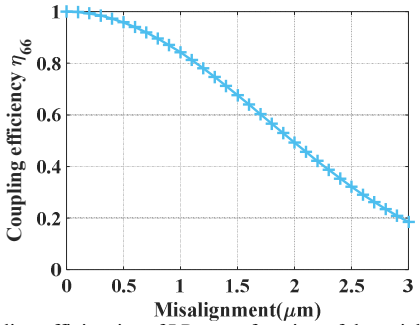

Fig.7. Coupling efficiencies of LP_{02} as a function of the axial misalignment.

Through the analysis of the above results, the variation rule of coupling efficiency between different modes under the conditions of axial misalignment d and the direction of the

misalignment θ is revealed, and the coupling efficiency of different modes had great differences.

IV. CONCLUSION

In this paper, a mathematical model of coupling efficiency of FMF fusion splice is established. The influence of axial misalignment and the direction of the misalignment parameters on coupling efficiency is studied by taking six-mode fiber as an example, and compared with the coupling efficiency of different spatial modes under the same influencing factors. This method can be used as a reference method to measure the accuracies of other higher-order mode approximate coupling efficiency models. Our future work will consider the effects of more complicated situations, including different FMF parameters, such as core radii, relative-index, normalized frequencies as well as profile shapes, on the coupling efficiency of FMF fusion splice. The research results can provide theoretical basis for high-sensitivity fault detection and FMF sensing.

ACKNOWLEDGMENT

This work was supported in part by the National Natural Science Foundation of China (62105246), Basic Research Project of Wenzhou (G20210010), Zhejiang Provincial Natural Science Foundation of China under Grant No. LY23F050003.

REFERENCES

[1] Georg Rademacher, Benjamin J. Puttnam, Ruben S. Luís, Jun Sakaguchi, Werner Klaus, Tobias A. Eriksson, Yoshinari Awaji, Tetsuya Hayashi, Takuji Nagashima, Tetsuya Nakanishi, Toshiki Taru, Taketoshi Takahata, Tetsuya Kobayashi, Hideaki Furukawa, and Naoya Wada. 10.66 Peta-Bit/s Transmission over a 38-Core-Three-Mode Fiber[C]. Optical Fiber Communication Conference, Optical Society of America, 2020: Th3H.1.

[2] Guifang Li, Neng Bai, Ningbo Zhao, Cen Xia. Space-division multiplexing: the next frontier in optical communication[J]. Advances in Optics and Photonics, 2014, 6(4): 413-487.

[3] Winzer P J. Making spatial multiplexing a reality[J]. Nature Photonics, 2014, 8(5): 345-348.

[4] Daiki Soma, Shohei Beppu, Noboru Yoshikane, and Takehiro Tsuritani. High-Capacity Mode Division Multiplexing Transmission Technology[C]. Optical Fiber Communication Conference, Optical Society of America, 2022: M4B.2.

[5] Wenping Zhang, Feng Liu, Zhengxing He, Lin Xu, and Guijun Hu. Fault detection performance of a multi-mode transmission reflection analysis for a few-mode fiber link[J]. Optics Letters, 2022, 47(1): 74-77.

[6] Atsushi Nakamura, Tomokazu Oda, and Daisuke Iida. Loss measurement of each mode in few-mode fiber links with crosstalk-inducing points based on optical time domain reflectometry[J]. Optics Express, 2020, 28(20): 30035-30047.

[7] Hiroshi Takahashi, Kunihiro Toge, Tomokazu Oda, and Tetsuya Manabe. Rayleigh-based OTDR with dynamic modal crosstalk suppression[J]. Optics Express, 2019, 27(2): 783-791.

[8] Atsushi Nakamura, Keiji Okamoto, Yusuke Koshikiya, and Tetsuya Manabe. Effective Mode Field Diameter for LP_{11} Mode and Its Measurement Technique [J]. IEEE Photonics Technology Letters, 2016, 28(22): 2553-2556.

[9] Loss Cause Identification by Evaluating Backscattered Modal Loss Ratio Obtained With 1-μm-Band Mode-Detection OTDR[J]. Journal of Lightwave Technology, 2016, 34(15): 3568-3576.

[10] He Zhenxing, Liu Feng, Zhang Wenping, Xu Lixin, and Hu Guijun. Analysis of characteristics of few-mode fiber fusion splicing under dynamic spatial mode crosstalk[J]. Applied Optics, 2021, 60(30): 9432-9439.

[11] Xingjie Fan , Dawei Wang , Julian Cheng , Jingkai Yang, and Jing Ma. Few-Mode Fiber Coupling Efficiency for Free-Space Optical Communication[J]. Journal of Lightwave Technology, 2021, 39(6): 1823-1829.